

Type equation here. **Rapid Chemoselective Bioconjugation Through the Oxidative Coupling of Anilines and Aminophenols**

Christopher R. Behrens,^a Jacob M. Hooker,^b Allie C. Obermeyer,^a Dante W. Romanini,^a
Elan M. Katz,^a and Matthew B. Francis^{a,c,*}

^aDepartment of Chemistry, University of California, Berkeley, California 94720-1460, ^bAthinoula A. Martinos Center for Biomedical Imaging, Department of Radiology, Massachusetts General Hospital, Harvard Medical School, Charlestown, MA 02129, ^cMaterials Sciences Division, Lawrence Berkeley National Laboratories, Berkeley, California 94720-1460.
francis@cchem.berkeley.edu

Supporting Information

Table of Contents	Page
S.1 Aminophenol/Aniline Coupling Small Molecule Model Reaction	S2
S.2 Crystal Formation for X-ray Analysis	S2
S.3 Proposed Mechanism of the Oxidative Coupling Reaction	S3
S.4 Production of Genome-Free MS2 Capsids	S3
S.5 Diazonium/Dithionite Modification Protocol for MS2	S4
S.6 Preparation of MS2-T19Y Mutants	S4
S.7 General Oxidative Coupling Procedure (written for the Oxidative Coupling of Aniline Peptide 17 to 11 (MS2- <i>o</i> -aminotyrosine-85))	S5
S.8 Synthesis of PEG- <i>o</i> -Aminophenol, PEG-Aniline, and Aniline Peptide	S5
S.9 Synthesis of Cyclic RGD Peptide Aminophenol and Subsequent Coupling of <i>p</i> -Toluidine	S7
S.10 Labeling of T19pAF N87C MS2 with IRDye 680LT Maleimide	S8
S.11 Size Exclusion Chromatography of MS2 and MS2 Conjugates	S9
S.12 Oxidative Coupling in the Presence of Glucose	S9
S.13 Reversed Phase HPLC of Small Molecule Coupling Reaction	S10
S.14 Coupling of <i>p</i> -toluidine to 11 (MS2- <i>o</i> -aminotyrosine-85)	S10
S.15 Preparation of Lysozyme-aniline and Coupling to PEG- <i>o</i> -aminophenol	S11
S.16 References	S12
S.17 NMR Spectra of 6a and High Resolution MS of Figure 2	S13
S.18 Crystallographic Characterization Data	S15

S1. Aminophenol/Aniline coupling small molecule model reaction.

Small molecule coupling reaction between p-toluidine and 2-amino-4-methylphenol

2-Amino-4-methylphenol (**4**, 123 mg, 1 mmol) and *p*-toluidine (**1a**, 107 mg, 1 mmol) were dissolved in two separate portions of acetonitrile (2 mL each) and then added to 2 L of 10 mM phosphate buffer, pH 6.5. Sodium periodate (2.14 g, 10 mmol) was dissolved in 20 mL of phosphate buffer and then added in one portion with vigorous stirring. The solution immediately turned red. After 5 min, sodium chloride was added to 1 M and the solution was extracted with 1 L portions of ethyl acetate until the organic layers showed no more color. The combined organic layers were washed with brine and dried over sodium sulfate before removing the solvent under reduced pressure. The resulting solid was purified via silica gel chromatography using a mobile phase of 1:1 ethyl acetate:hexanes ($R_f \approx 0.25$) to afford 95 mg of **6a** as a gray powder (40% yield). ESI-MS: 242.7 (242.27 expected). ^1H NMR (300 MHz, CD_3CN) δ 1.6 (s, 3H), 2.3 (s, 3H), 3.0-3.1 (dd, 2H), 5.2 (s, 1H), 7.1 (d, 2H), 7.2 (d, 2H), 7.5 (br s, 1H). ^{13}C NMR (100 MHz, CD_3CN) δ 19.82, 22.68, 27.43, 80.12, 83.86, 115.64, 120.53, 129.93, 134.61, 136.95, 166.34, 171.83. ^1H and ^{13}C NMR spectra can be found in Figure S9. IR: 3250, 3048, 2218, 1713, 1616 cm^{-1} .

Small molecule coupling reaction between p-toluidine and 2-hydroxy-4-methylphenol

In the above reaction, byproduct **5a** was not produced in sufficient yield for characterization using NMR. Instead the reaction between *p*-toluidine and 2-hydroxy-4-methylphenol was used to produce **5a** directly. Co-injection on reversed phase HPLC showed the major product of this reaction matched the **5a** byproduct observed in the above reaction. The mass spectra of the two compounds were identical, and both compounds exhibited the same gain of 2 Da when exposed to TCEP. The synthesis of **5a** was achieved as follows:

2-hydroxy-4-methylphenol (12 mg, 0.097 mmol) and *p*-toluidine (**1a**, 9 mg, 0.084 mmol) were dissolved in acetonitrile (0.2 mL) and then diluted with 6 mL of water. Sodium periodate (52 mg, 0.24 mmol) was dissolved in 2 mL of water and then added to the stirring solution in one portion. The solution immediately turned a deep purple. After 5 minutes, the water was removed *in vacuo*. The resulting red solid was taken up directly in CDCl_3 for analysis. IR (thin film): 3268, 3034, 2923, 2854, 1712, 1674, 1637, 1608, 1515 cm^{-1} . ^1H NMR (600 MHz, CDCl_3) δ 7.19 (d, 2H), 6.77 (br s, 2H), 6.61 (br s, 1H), 6.34 (br s, 1H), 4.29 (br s, 1H), 2.37 (s, 3H), 2.34 (d, 3H). ^{13}C NMR (150 MHz, CDCl_3) δ 18.46, 21.13, 101.09, 120.53, 127.50, 129.72, 135.52, 147.87, 153.14, 158.73, 182.92. One ^{13}C NMR signal was not detected, possibly due to rapid tautomerization of the molecule. HRMS (ESI) calculated for $\text{C}_{14}\text{H}_{14}\text{O}_2\text{N}$ ($[\text{M}+\text{H}]^+$) 228.1021, found 228.1024. HRMS (ESI) calculated for $\text{C}_{14}\text{H}_{13}\text{O}_2\text{N}^{23}\text{Na}$ ($[\text{M}+\text{Na}]^+$) 250.0839, found 250.0840.

S2. Crystal formation for X-ray analysis.

6a was dissolved in a minimal amount of acetonitrile and then diluted to approximately 1 mg/mL with toluene. Crystals formed overnight upon vial-in-vial vapor diffusion using hexanes as the diluting solvent.

A colorless rod measuring 0.12 x 0.10 x 0.10 mm in size was mounted on a Cryoloop with Paratone oil. Data were collected in a nitrogen gas stream at 100(2) K using phi and omega scans. The

crystal-to-detector distance was 60 mm and the exposure time was 5 s per frame using a scan width of 1.0°. Data collection was 98.3% complete to 67.00° in θ . A total of 17398 reflections were collected covering the indices, $-16 \leq h \leq 16$, $-8 \leq k \leq 7$, $-16 \leq l \leq 16$. 2246 reflections were found to be symmetry independent, with an R_{int} of 0.0248. Indexing and unit cell refinement indicated a primitive, monoclinic lattice. The space group was found to be P2(1)/c (No. 14). The data were integrated using the Bruker SAINT software program and scaled using the SADABS software program. Solution by direct methods (SIR-2008) produced a complete heavy-atom phasing model consistent with the proposed structure. All non-hydrogen atoms were refined anisotropically by full-matrix least-squares (SHELXL-97). All hydrogen atoms were placed using a riding model. Their positions were constrained relative to their parent atoms using the appropriate HFIX command in SHELXL-97.

S3. Proposed mechanism of oxidative coupling reaction.

Our proposed mechanism for the oxidative coupling reaction presented in this paper contains two overall steps. First, the aniline attacks an iminoquinone intermediate to form the proposed A+B intermediate. The second step involves a second oxidation to the iminoquinone followed by two competing routes that lead to either **5a** or **6a**. In route A, hydrolysis of the imine results in **5a**, which cannot be further oxidized. In route B, hydration of the ketone, imino alcohol cleavage by the periodate, and finally 1,4 conjugate addition results in **6a**. This seems to be the most plausible route to **6a**, but there are several alternative mechanisms - a detailed mechanistic study is necessary to determine the correct one. We have also observed that further oxidation of **5a** does not result in any conversion to **6a**.

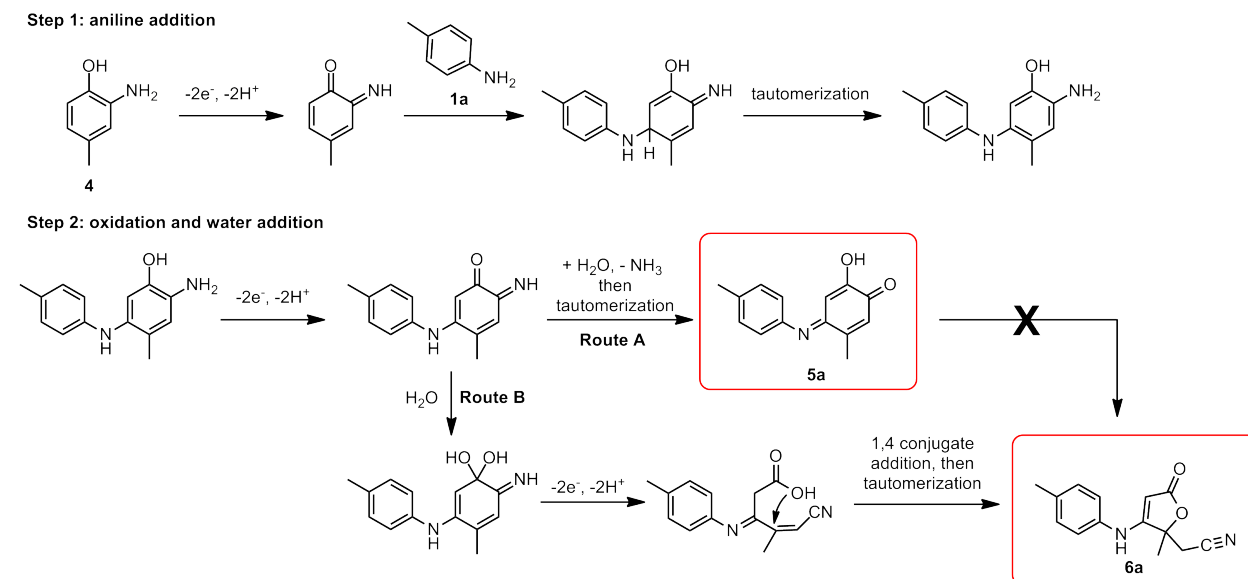


Figure S1. Proposed mechanism for aniline addition to aminophenol under oxidative conditions. Step 1 shows the aniline addition and step 2 shows two possible water addition routes that result in either product **5a** or **6a**. **5a** cannot be converted to **6a** once formed.

S4. Production of genome-free MS2 capsids.

The DNA encoding the MS2 coat protein sequence was inserted into the pBAD/*Myc*-His vector. The plasmid was transformed into New England Biosciences 5 α *E. coli* and grown in LB media with 100

$\mu\text{g/mL}$ ampicillin and 0.05% arabinose for induction. After 18 h of growth at 37 °C the cells were centrifuged and separated from the media. The following steps were carried out at 4 °C: First, the cells were resuspended in pH 9 taurine buffer, lysed via sonication, and then the cell lysate was centrifuged and the supernatant was loaded on a DEAE-Sephadex column (GE Healthcare). Fractions containing MS2 capsids were combined and the protein was precipitated by adding $(\text{NH}_4)_2\text{SO}_4$ to a final concentration of 50%. The protein pellet was next resuspended in a minimal volume of pH 6.5 phosphate buffer and applied to a Sephacryl-500 column (GE Healthcare). Fractions containing MS2 capsids were combined and concentrated using 100k MWCO spin concentrators (Millipore).

Both wild type (19T and 85Y) MS2 and T19Y MS2 were produced using this procedure. T19pAF MS2 was produced as described in Supporting Information Reference [1].

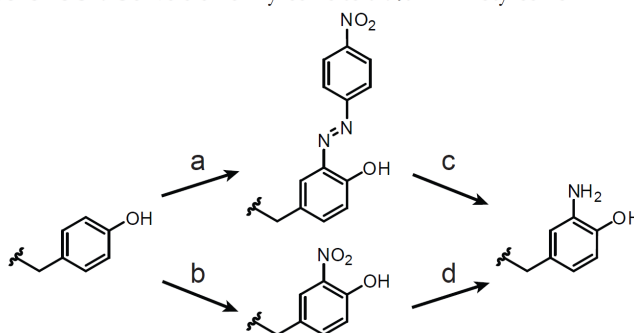
S5. Diazonium/dithionite modification of MS2 to produce 11 (MS2-*o*-aminotyrosine-85).

4-Nitrobenzenediazonium tetrafluoroborate (Sigma-Aldrich) was dissolved in acetonitrile at a concentration of 200 mM and stored on ice. To a 495 μL solution of wild type MS2 capsids (100 μM in monomer) in 75 mM phosphate buffer, pH 9, was added 5 μL of the diazonium solution (resulting in a final concentration of 2 mM diazonium salt). The solution was allowed to react for 15 min while being cooled on ice before purification on a Nap-5 Sephadex size exclusion column equilibrated with pH 6.5 phosphate buffer. For other proteins, we recommend varying the concentrations of the diazonium salt to obtain the optimal level of conversion and maximum protein recovery.

To the above solution of azo-modified MS2 was added sodium dithionite (Supporting Information Reference [2]) to a final concentration of 20 mM. This solution was allowed to react for 90 minutes at room temperature before purification on a Nap-10 Sephadex size exclusion column (GE Healthcare) equilibrated with pH 6.5 phosphate buffer. For MS2 capsids, the total protein recovery was ~70% after both reaction steps and SEC columns.

Note: It is important that a fresh bottle of sodium dithionite that has been stored at 4 °C is used. Reduction using some samples of sodium dithionite that had been stored at room temperature resulted in additional unidentified products (such as [M+80]) being formed in varying amounts.

Scheme S1. Conversion of Tyrosine to *ortho*-Aminotyrosine^a



^aConditions: (a) 4-nitrobenzenediazonium tetrafluoroborate, pH 9, 4 °C, 15 min; (b) $\text{C}(\text{NO}_2)_4$, pH 8, 90 min; (c) $\text{Na}_2\text{S}_2\text{O}_4$, pH 7, 1 h; (d) $\text{Na}_2\text{S}_2\text{O}_4$, pH 7, 15 min.

S6. Generation of MS2 T19Y mutants.

The QuikChange II Site Directed Mutagenesis Kit (Stratagene, La Jolla, CA) was used to mutate the threonine at position 19 to a tyrosine using the following forward and reverse primers:

Forward: 5' - ggaactggcgacgtgtatgtcgccca - 3'

Reverse: 5' - ttgctggggcgacatacacgtcgcca - 3'

The manufacturer's instructions were followed for these procedures. Incorporation of the point mutation was confirmed by sequencing of the colonies that were obtained after the mutation procedure.

S7. General procedure for coupling anilines to *o*-aminophenols on proteins (written specifically for the oxidative coupling of aniline peptide **17** to **11** (MS2-*o*-aminotyrosine-85)).

To a solution of **11** (50 μ M) in dilute pH 6.5 phosphate buffer was added a solution of aniline-His₆-Gly peptide (**17**) to a final concentration of approximately 500 μ M. Sodium periodate (Sigma-Aldrich) was dissolved to a concentration of 50 mM in dilute pH 6.5 phosphate buffer. It was then added to the protein solution to reach a final concentration of 5 mM, and the reaction was allowed to proceed for 2 min at RT. In cases where a reaction quench was desired, a 100 mM solution of tris(carboxyethyl)phosphine (TCEP) at pH 6.5 was added to a final concentration of 50 mM. The resulting protein samples were purified on a Nap 5 Sephadex size exclusion column (GE Healthcare). If any unreacted peptide remained, it was removed by diluting the protein solution with phosphate buffer and concentrating the resulting solution using a 100k molecular weight cut-off spin concentrator (Millipore).

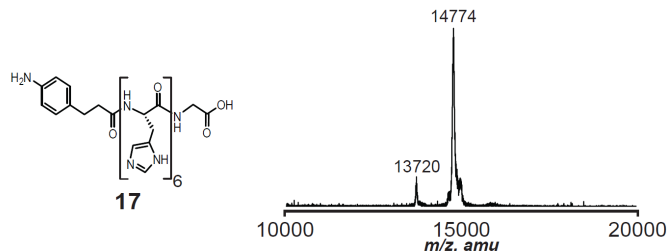


Figure S2. MS2-*o*-aminophenol-85 (**11**, 50 μ M) was reacted with **17** (500 μ M) in the presence of sodium periodate (5 mM) for 2 minutes before purification by size exclusion chromatography (NAP-5 column). SDS-PAGE analysis of this sample appears in the main text, Figure 4c, lane 8.

S8. Synthesis of PEG-*o*-aminophenol, PEG-aniline, and aniline peptide.

Monomethoxy-polyethyleneglycol-o-aminophenol (5k-PEG-*o*-aminophenol **13**). Dicyclohexylcarbodiimide (27 mg, 0.13 mmol) was added to a flask containing 3-(4-hydroxy-3-nitrophenyl)propionic acid (23 mg, 0.11 mmol, synthesized via procedure from Supporting Information Reference [4]) and *N*-hydroxysuccinimide (13 mg, 0.11 mmol) dissolved in CH₂Cl₂. The reaction was stirred for 15 min at room temperature, after which the solution was filtered to remove the DCU precipitate. The resulting solution was added to a second flask containing monomethoxy-polyethyleneglycol-amine (Sigma-Aldrich, 5000 molecular weight, 500 mg, 0.10 mmol) and triethylamine (0.32 mmol). After 2 h of stirring at RT the solvent was removed under reduced pressure and the resulting solid was dissolved in 15 mL of pH 6.5 100 mM phosphate buffer. The resulting suspension was then filtered to remove insoluble

material. Sodium dithionite (1 mmol, see storage Note in Section S5, above) was then added and solution immediately turned colorless. After 5 min of stirring, NaCl was added to 2 M and the aqueous layer was extracted three times with CH₂Cl₂. The combined organic extracts were washed once with brine and dried over Na₂SO₄. The solvent was removed under reduced pressure to afford 250 mg of product as a solid (48% yield for **13**). The extent of PEG modification with *o*-aminophenol was quantified by the absorbance at 290 nm and compared to standards of *o*-amino-*p*-cresol. This value was used to determine the amount of functionalized PEG that was added to the coupling experiments. 2k-PEG-*o*-aminophenol **14** was prepared using the same procedure and purification protocol. The product was obtained as a solid (~25% yield). The extent of conversion for the 2k product was determined as described for PEG **13**, above.

Monomethoxy-polyethyleneglycol-aniline (5k-PEG-aniline 15). Dicyclohexylcarbodiimide (27 mg, 0.13 mmol) was added to a flask containing 3-(4-(*N*-*boc*-amino)phenyl)propionic acid (29 mg, 0.11 mmol) and *N*-hydroxysuccinimide (13 mg, 0.11 mmol) dissolved in CH₂Cl₂. The reaction was stirred for 15 min at room temperature, after which the solution was filtered to remove the DCU precipitate. The resulting material was added to a second flask containing monomethoxy-polyethyleneglycol-amine (Sigma-Aldrich, 5000 molecular weight, 500 mg, 0.10 mmol) and triethylamine (0.32 mmol). After two hours of stirring at room temperature, the solvent was removed under reduced pressure. The resulting solid was dissolved in 15 mL of 1 M NaCl and filtered to remove insoluble material. The aqueous layer was extracted three times with CH₂Cl₂ and the combined organic extracts were washed once with brine and dried over Na₂SO₄. The resulting solid was dissolved in 10 mL of CH₂Cl₂ and 10 mL of trifluoroacetic acid and allowed to react for 1 h at room temperature. The solvents were next removed under reduced pressure. The residue was dissolved in phosphate buffer and adjusted to pH 8. NaCl was added to 2 M and the aqueous layer was extracted with CH₂Cl₂ and dried as described above. Removal of the solvent under reduced pressure afforded 240 mg of solid (46% yield). The extent of PEG modification with aniline was quantified by absorbance at 287 nm and compared to standards of *p*-toluidine. This value was used to determine the amount of functionalized PEG that was added to the coupling experiments. 2k-PEG-aniline **16** was prepared using the same procedure and purification protocol. The product was obtained as a solid (~25% yield). The extent of conversion for the 2k product was determined as described for PEG **15**, above.

Aniline-His₆-Gly peptide 17. The peptide was synthesized using standard Fmoc chemistry using a Wang resin preloaded with glycine (EMD Chemicals). HCTU was used as a coupling agent. As a final step, the N-terminus of the peptide was modified with the NHS ester of 3-(4-(*N*-*boc*-amino)phenyl)propionic acid, which was prepared as described in the PEG-aniline (**15**) synthesis described above. After cleavage from the resin the peptide was precipitated by the addition of ether, isolated via filtration, and then dissolved in water for use in the coupling reactions. The peptide was characterized using MALDI-TOF with sinapinic acid as the matrix.

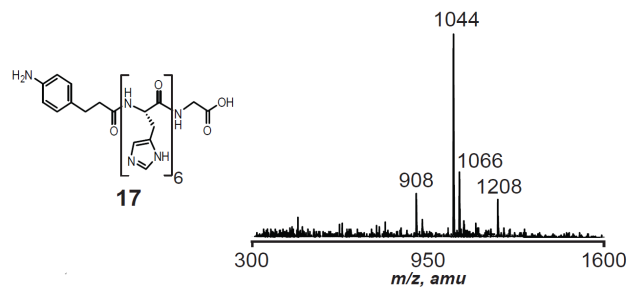


Figure S3. MALDI-TOF of **17** after cleavage from resin. Expected: $[M+H]^+ = 1045$, $[M+Na]^+ = 1067$ *m/z*.

S9. Synthesis of cyclic RGD peptide aminophenol and subsequent coupling of *p*-toluidine.

Cyclic peptide RGDyE (Peptides International, structure in Figure S4) was dissolved in DMSO to a concentration of 50 mg/mL, then diluted to 5 mM in pH 6.5 phosphate buffer (10 mM). A 50 μ L portion of this peptide solution was diluted into 400 μ L of 50 mM pH 7.8 ammonium bicarbonate buffer. To this solution was added 50 μ L of a 150 mM solution of tetranitromethane dissolved in ethanol (Scheme S1). After 1.5 h reaction at room temperature trifluoroacetic acid was added to achieve a pH of 3 and the solution was loaded on to a C18 Sep Pack (Waters) pre-conditioned with acetonitrile then 0.1% aqueous TFA. After washing with aqueous 0.1% TFA the peptide was eluted with acetonitrile. After removing the acetonitrile under reduced pressure the solid peptide was dissolved in 100 μ L pH 6.5 phosphate buffer (10 mM). The nitrated peptide was characterized by MALDI-TOF MS using sinapinic acid as the matrix. In addition to the expected peak at 666 amu there was a second peak at 650 amu (-16 amu from the main peak) that was an artifact seen on MALDI-TOF MS for all nitrophenol containing substrates (Figure S4c). Sodium dithionite dissolved in pH 6.5 phosphate buffer (200 mM) was added to 20 μ L of the above peptide solution to a final concentration of 5 mM. After 15 minutes at room temperature 2 μ L were removed for MS characterization and the remainder was added to a solution of *p*-toluidine (200 μ M). Sodium periodate was added to a final concentration of 5 mM and after two minutes of reaction the solution was purified via C18 Zip Tip (Millipore) in the same manner as the C18 Sep Pack above. The RGD-toluidine coupling product was characterized via LCMS. In addition to the expected mass of 755 amu, a second peak at 740 amu was observed. This mass corresponded to product **5**, in which the aniline and aminophenol have formed a covalent bond but imine hydrolysis occurred before the iminoalcohol cleavage. This peak becomes the major peak when reaction-limiting concentrations of sodium periodate are used (Figure S4g). Also, when TCEP was added, the mass corresponding to **5** increased by two mass units, thus mimicking the behavior of **5a** (Figure S4e and S4f, for with and without TCEP, respectively).

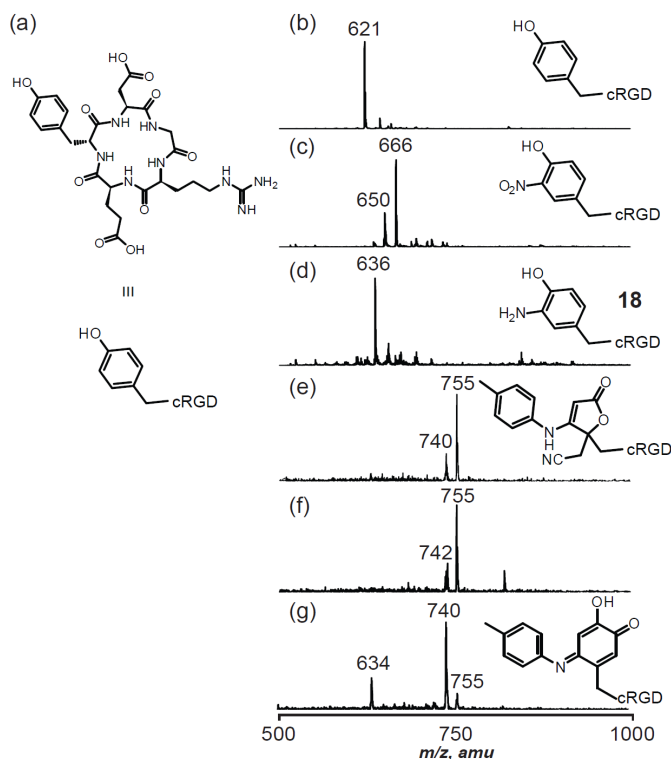


Figure S4. Modification of cyclic RGDyE peptide to aminophenol cyclic RGD. (a) Cyclic RGDyE and abbreviated structure. (b) MALDI-TOF MS of unmodified RGDyE. Expected: $[M+H]^+ = 621$. (c) MS after reaction with tetranitromethane at pH 7.8 for 1 h. Expected: $[M+H]^+ = 666$. The peak at 650 amu (loss of 16 from main peak) is an artifact always seen in the MALDI-TOF MS of nitrophenol substrates. (d) MS after reduction of nitro-RGD with sodium dithionite at pH 6.5 for 15 min. Expected: $[M+H]^+ = 636$. (e) LC-ESI-MS of coupling between **18** and toluidine (200 μ M) in the presence of sodium periodate (5 mM) at pH 6.5. Expected: $[M+H]^+ = 755$, $[m+H]^+ = 740$. (f) Addition of TCEP to sample e immediately prior to injection on LC-ESI-MS shows an addition of two mass units to the minor product, thus mimicking the behavior of **5a**. Expected: $[M+H]^+ = 755$, $[m+H_2+H]^+ = 742$. (g) MS of coupling between **18** and toluidine (200 μ M) at pH 6.5 in the presence of a reaction-limiting concentration of sodium periodate. The mass at 740 m/z corresponds to that of **5**.

S10. Labeling of T19pAF N87C MS2 with IRDye 680LT maleimide.

MS2 capsids with the unnatural amino acid *p*-aminophenylalanine at position 19 and cysteine at position 87 were cloned, expressed, and purified as described in Supporting Information Reference [3]. The interior cysteine at position 87 was then modified with IRDye 680LT maleimide (LI-COR). To MS2 capsids (100 μ M) in pH 6.5 phosphate buffer was added IRDye 680LT maleimide to a final concentration of 1 mM. After 1 h of reaction at room temperature the protein was purified via a Nap 5 size exclusion column, followed by a Nap 10 size exclusion column (GE Healthcare). The solution was then concentrated using a 100k molecular weight cutoff spin concentrator (Millipore). After concentration the solution was diluted with pH 6.5 phosphate buffer and concentrated again. This process was repeated until the flow through from the spin concentrator showed no signs of free dye. The capsids were then

disassembled and analyzed via SDS-PAGE gel with both fluorescence detection and Coomassie staining (Figure 5b).

S11. Size exclusion chromatography of unmodified MS2 capsids and MS2 capsid conjugates.

The capsids were analyzed by size exclusion chromatography to verify their assembly state after conjugation to peptides or PEG chains. MS2 was labeled with IRDye 680LT (LI-COR) on the inner surface using maleimide chemistry and then further modified on the outer surface via oxidative coupling chemistry. The MS2-IRDye 680LT (no outer surface modification), MS2-IRDye 680LT/cRGDyE conjugate, and MS2-IRDye 680LT/PEG5k conjugate were injected onto a GF-250 size exclusion column (Agilent). The mobile phase (0.5 mL/min flowrate) was 100 mM phosphate buffer pH 6.5. Each sample eluted in the void volume of the column, which suggested all samples were still in the assembled capsid form (Figure S5).

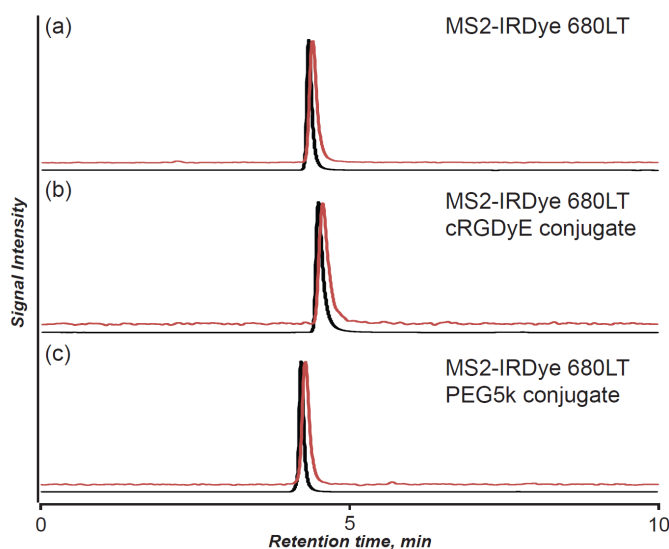


Figure S5. Size exclusion chromatography of MS2 capsids on GF-250 column (Agilent) to verify that disassembly did not occur. Intact capsids elute at 4-5 min, while disassembled monomer elute at 8-10 min. The black trace is the absorbance at 280 nm and the red trace is the fluorescence (680 nm excitation, 700 nm emission) of IRDye 680LT (LI-COR), which has been attached to the inner surface of the capsids. The retention time difference between the black and red traces corresponds to the distance between the two detectors. (a) MS2 capsid with IRDye 680LT and no outer surface modification. (b) MS2-IRDye 680LT with cRGDyE conjugated to the outer surface. (c) MS2-IRDye 680LT with PEG (5k molecular weight) conjugated to the outer surface. These samples correspond to those analyzed in the gel shown in figure 5b.

S12. Oxidative coupling in the presence of glucose.

Sodium periodate can also be used as an oxidant for the cleavage of vicinal diols in sugars. As a preliminary test for the compatibility of this oxidative coupling reaction with carbohydrates, we repeated the coupling of PEG-aminophenol (**13**) with T19pAF MS2 (**7**) in the presence of varying amounts of glucose. We found no significant difference in coupling between samples with 0 or 20 mM glucose (Figure S6). Though this experiment did not analyze the state of the vicinal diols, it did show that small

amounts of sugars will not consume enough oxidative equivalents of periodate to prevent the aminophenol-aniline coupling.

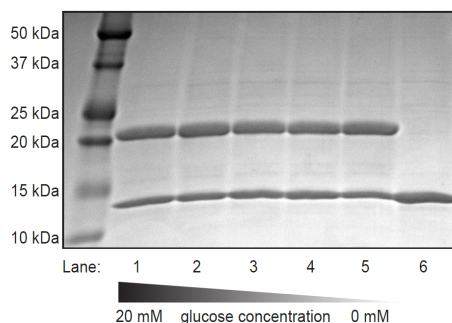


Figure S6. Attachment of PEG aminophenol (5k molecular weight) to T19 p AF MS2 in the presence of varying amounts of glucose. Compound **13** (200 μ M) was exposed to T19 p AF MS2 (30 μ M) for 5 min in the presence of sodium periodate (5 mM) and 20 mM, 5 mM, 2 mM, or 200 μ M glucose (Lanes 1-4, respectively). None show an appreciable difference from Lane 5 which had no glucose. Lane 6 is a negative control with 5 mM sodium periodate and 5 mM glucose but no **13**.

S13. Reversed phase HPLC of small molecule coupling reaction.

The isolated product **6a** and crude reaction of 2-amino-4-methylphenol (**4**) and *p*-toluidine (**1a**) were analyzed by reversed-phase HPLC on an Agilent 1100 Series HPLC System (Agilent Technologies, Santa Clara, CA). Reversed-phase liquid chromatography was accomplished on a Gemini 5 μ m C18 column (150 mm \times 4.6 mm, Phenomenex). The mobile phase (0.5 mL/min flowrate) was a linear gradient over 20 minutes from 15% to 95% acetonitrile:water containing 0.1% TFA.

S14. Coupling of *p*-toluidine to **11** (MS2-*o*-aminotyrosine-85).

11 was produced according to the procedure in section S5. **11** was then reacted with *p*-toluidine in the presence of sodium periodate. The capsids were disassembled before analysis by MALDI-TOF MS (Figure S7).

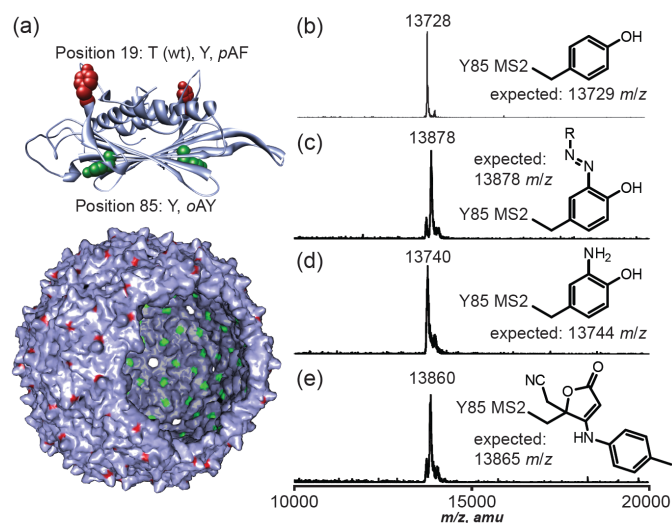


Figure S7. (a) Structure of the MS2 viral capsid (based on wt structure PDBID: 2MS2) indicating the locations of position 19 (outer surface) and 85 (inner surface). Following chemical modification, the capsids were dissociated and analyzed using MALDI-TOF MS: (b) wtMS2, (c) wtMS2 after reaction with 4-nitrobenzenediazonium tetrafluoroborate, (d) azo-modified MS2 after reduction with sodium dithionite, and (e) MS2-*o*-aminotyrosine-85 coupled to *p*-toluidine in the presence of 5 mM periodate (RT, 2 min).

S15. Preparation of lysozyme-aniline and subsequent coupling to PEG-*o*-aminophenol

3-(4-aminophenyl)propionic acid (Aldrich) was dissolved to 50 mM in DMF. N-hydroxysuccinimide was added to a concentration of 100 mM, after which 1-ethyl-3-(3-dimethylaminopropyl)carbodiimide (EDC, Fluka) was added to a concentration of 100 mM. After 10 min, a 50 μ L aliquot of the solution was added to 950 μ L of a 10 μ M solution of lysozyme (from chicken egg white, Sigma) in 50 mM pH 8.5 phosphate buffer. The resulting solution was allowed to react at room temperature for 1 h, at which time the lysozyme was purified via a Nap-10 size exclusion column equilibrated with pH 6.5 phosphate buffer. After concentrating the lysozyme down to a volume of 1.0 mL using a 10kDa molecular weight cutoff spin concentrator, it was again purified through a Nap-10 size exclusion column. MALDI-TOF analysis indicated a range of two to five aniline modifications on each lysozyme (Figure S8).

The resulting lysozyme-aniline (20 μ M) was reacted with PEG2k-aminophenol (100 μ M), **14**, in the presence of NaIO₄ (2 mM) for 2 min. The reaction was quenched with DTT and was analyzed via SDS-PAGE (Figure S8c).

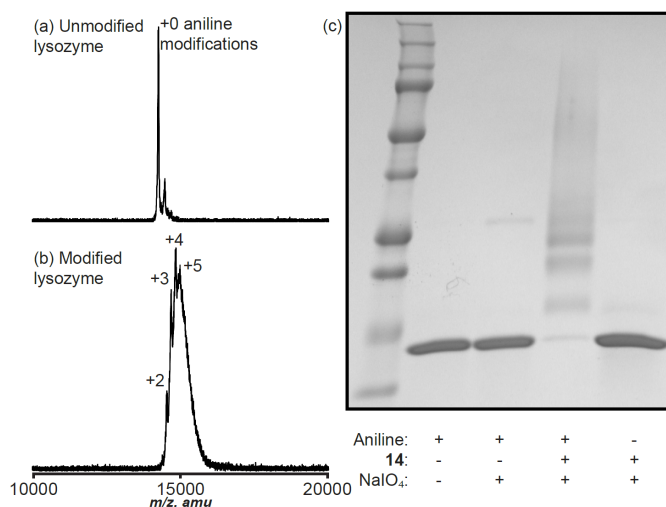


Figure S8. (a) MALDI-TOF of wildtype lysozyme. (b) MALDI-TOF of lysozyme modified with 3-(4-aminophenyl)propionic acid showed 2-5 aniline modifications. (c) SDS-PAGE analysis of lysozyme (20 μM) reacted with PEG2k-aminophenol (**14**, 100 μM) in the presence of NaIO₄ (2 mM) for 2 min. The reaction only occurred if both the aniline and the aminophenol were present.

S16. References.

- [1] Carrico, Z. M., Romanini, D. W.; Mehl, R. A.; Francis, M. B. *Chemical Communications* **2008**, *10*, 1205-1207.
- [2] Gorecki, M.; Wilchek, M.; Patchornik, A. *Biochimica et Biophysica Acta* **1971**, *229*, 590-595.
- [3] Tong, G. J., Hsaio, S. C., Carrico, Z. M., Francis, M. B. *Journal of the American Chemical Society* **2009**, *131*, 11174-11178
- [4] Wright, J.B. *Journal of Heterocyclic Chemistry* **1972**, *9*, 681-682

S17. NMR Spectra of 6a and High Resolution MS of Figure 2

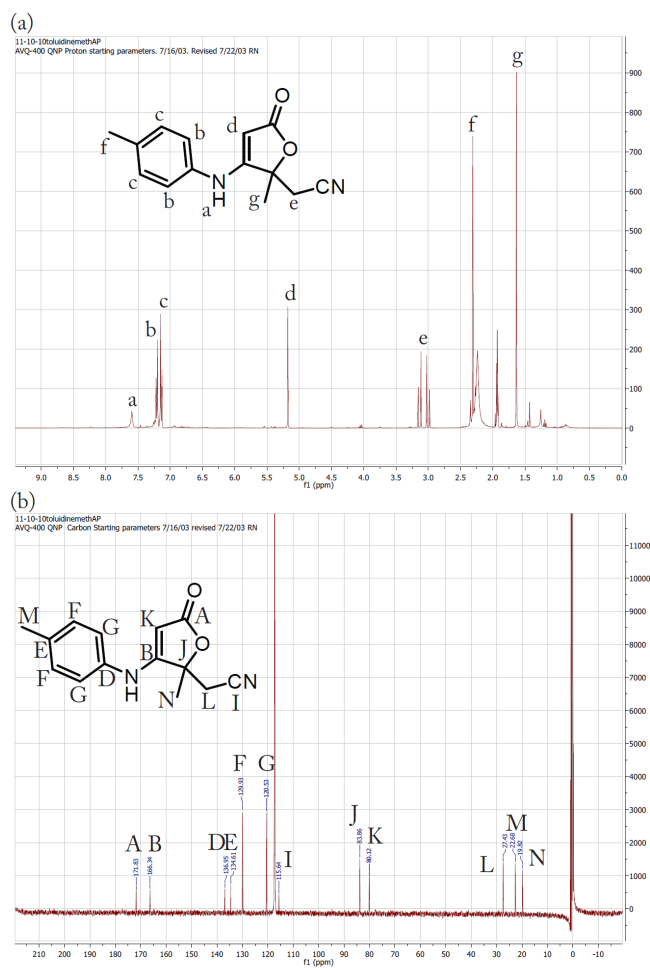


Figure S9. (a) ^1H NMR (300 MHz, CD_3CN) of **6a** (b) ^{13}C NMR (100 MHz, CD_3CN) of **6a**

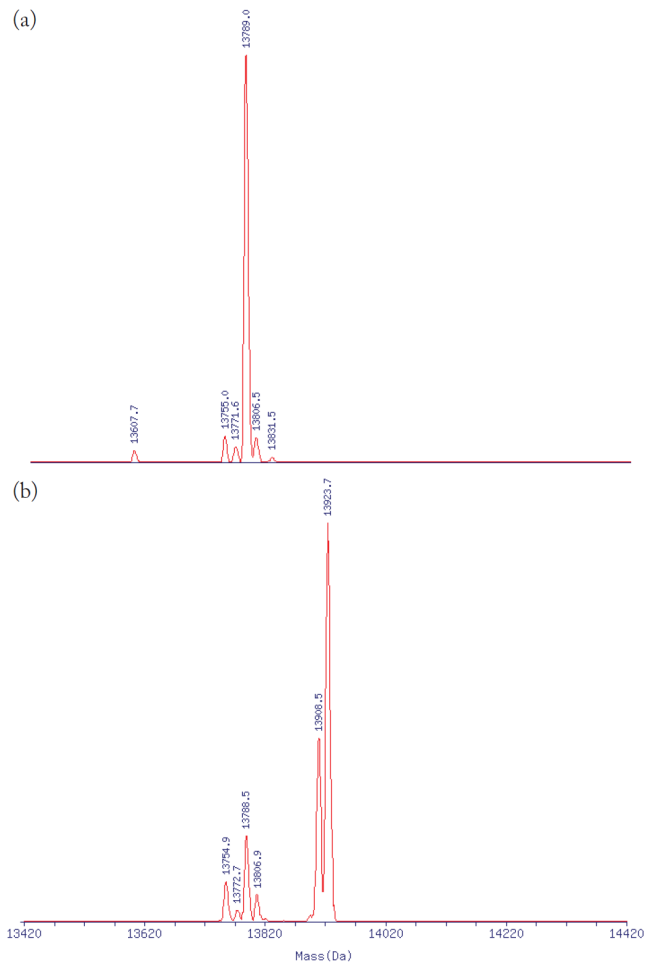
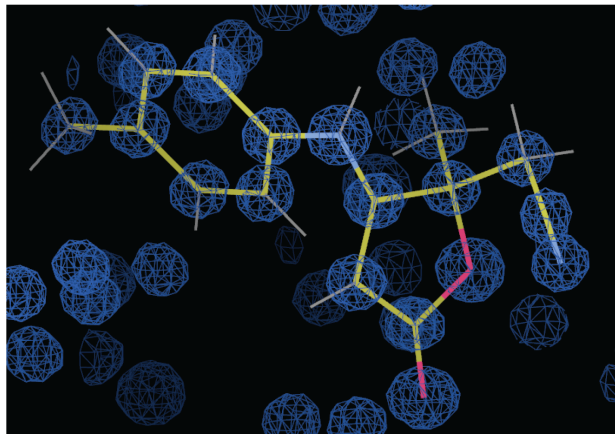


Figure S10. (a) Unmodified T19pAF MS2 capsids were disassembled into monomers and analyzed via ESI-MS. (b) T19pAF MS2 (30 μ M) was reacted with 2-amino-4-methylphenol (100 μ M) in the presence of NaIO₄ (1 mM) for 30 s before quenching with 50 mM tris(2-carboxyethyl)phosphine (TCEP). The product was purified with size exclusion chromatography, the capsids were disassembled into monomers, and the protein was analyzed via ESI-MS.

S18. Crystallographic Characterization Data.

(a)



(b)

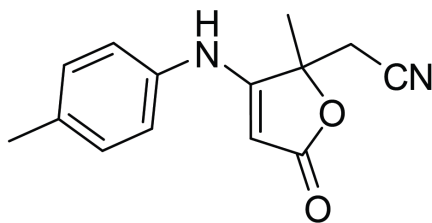


Figure S11. (a) **6a** structure overlay with electron density map. (b) Structure of **6a**.

Table 1. Crystal data and structure refinement for **6a**.

X-ray ID	6a	
Empirical formula	C ₁₄ H ₁₄ N ₂ O ₂	
Formula weight	242.27	
Temperature	100(2) K	
Wavelength	1.54178 Å	
Crystal system	Monoclinic	
Space group	P2(1)/c	
Unit cell dimensions	a = 14.1010(12) Å	$\alpha = 90^\circ$.
	b = 6.9117(5) Å	$\beta = 112.570(5)^\circ$.
	c = 14.0777(12) Å	$\gamma = 90^\circ$.
Volume	1266.96(18) Å ³	
Z	4	
Density (calculated)	1.270 Mg/m ³	
Absorption coefficient	0.701 mm ⁻¹	

F(000)	512
Crystal size	0.12 x 0.10 x 0.10 mm ³
Crystal color/habit	colorless rod
Theta range for data collection	3.39 to 67.64°.
Index ranges	-16<=h<=16, -8<=k<=7, -16<=l<=16
Reflections collected	17398
Independent reflections	2246 [R(int) = 0.0248]
Completeness to theta = 67.00°	98.3 %
Absorption correction	Semi-empirical from equivalents
Max. and min. transmission	0.9332 and 0.9206
Refinement method	Full-matrix least-squares on F ²
Data / restraints / parameters	2246 / 0 / 165
Goodness-of-fit on F ²	1.050
Final R indices [I>2sigma(I)]	R1 = 0.0674, wR2 = 0.1819
R indices (all data)	R1 = 0.0735, wR2 = 0.1872
Largest diff. peak and hole	0.682 and -0.304 e.Å ⁻³

Table 2. Atomic coordinates ($\times 10^4$) and equivalent isotropic displacement parameters ($\text{\AA}^2 \times 10^3$) for **6a**. $U(\text{eq})$ is defined as one third of the trace of the orthogonalized U^{ij} tensor.

	x	y	z	$U(\text{eq})$
C(1)	1035(2)	6562(3)	9080(2)	32(1)
C(2)	2165(2)	6529(3)	9760(2)	29(1)
C(3)	2482(2)	4657(4)	9937(2)	30(1)
C(4)	1627(2)	3432(3)	9422(2)	31(1)
C(5)	832(2)	7422(4)	8019(2)	38(1)
C(6)	1352(3)	6375(5)	7484(2)	47(1)
C(7)	373(2)	7526(4)	9582(2)	40(1)
C(8)	3726(2)	8466(3)	10631(2)	31(1)
C(9)	4047(2)	9883(4)	11390(2)	36(1)
C(10)	5086(2)	10239(4)	11916(2)	41(1)
C(11)	5832(2)	9183(4)	11716(2)	40(1)
C(12)	5490(2)	7773(4)	10956(2)	40(1)
C(13)	4459(2)	7416(4)	10414(2)	37(1)
C(14)	6958(3)	9555(5)	12282(3)	54(1)
N(1)	1775(3)	5490(5)	7072(2)	64(1)
N(2)	2660(2)	8206(3)	10066(2)	33(1)
O(1)	764(1)	4537(2)	8930(1)	32(1)
O(2)	1538(2)	1684(2)	9349(2)	37(1)

Table 3. Bond lengths [Å] and angles [°] for **6a**.

C(1)-O(1)	1.445(3)	C(8)-C(9)	1.390(4)
C(1)-C(2)	1.513(4)	C(8)-C(13)	1.390(4)
C(1)-C(7)	1.522(4)	C(8)-N(2)	1.417(3)
C(1)-C(5)	1.529(4)	C(9)-C(10)	1.386(4)
C(2)-N(2)	1.336(3)	C(9)-H(9)	0.9500
C(2)-C(3)	1.360(3)	C(10)-C(11)	1.395(4)
C(3)-C(4)	1.423(4)	C(10)-H(10)	0.9500
C(3)-H(3)	0.9500	C(11)-C(12)	1.389(4)
C(4)-O(2)	1.215(3)	C(11)-C(14)	1.501(4)
C(4)-O(1)	1.378(3)	C(12)-C(13)	1.380(4)
C(5)-C(6)	1.433(4)	C(12)-H(12)	0.9500
C(5)-H(5A)	0.9900	C(13)-H(13)	0.9500
C(5)-H(5B)	0.9900	C(14)-H(14A)	0.9800
C(6)-N(1)	1.154(4)	C(14)-H(14B)	0.9800
C(7)-H(7A)	0.9800	C(14)-H(14C)	0.9800
C(7)-H(7B)	0.9800	N(2)-H(2)	0.8800
C(7)-H(7C)	0.9800		
O(1)-C(1)-C(2)	103.49(19)	C(4)-C(3)-H(3)	125.7
O(1)-C(1)-C(7)	108.5(2)	O(2)-C(4)-O(1)	117.7(2)
C(2)-C(1)-C(7)	113.5(2)	O(2)-C(4)-C(3)	132.4(2)
O(1)-C(1)-C(5)	107.0(2)	O(1)-C(4)-C(3)	109.8(2)
C(2)-C(1)-C(5)	112.3(2)	C(6)-C(5)-C(1)	112.1(2)
C(7)-C(1)-C(5)	111.4(2)	C(6)-C(5)-H(5A)	109.2
N(2)-C(2)-C(3)	132.2(2)	C(1)-C(5)-H(5A)	109.2
N(2)-C(2)-C(1)	118.9(2)	C(6)-C(5)-H(5B)	109.2
C(3)-C(2)-C(1)	108.8(2)	C(1)-C(5)-H(5B)	109.2
C(2)-C(3)-C(4)	108.5(2)	H(5A)-C(5)-H(5B)	107.9
C(2)-C(3)-H(3)	125.7	N(1)-C(6)-C(5)	178.1(3)

C(1)-C(7)-H(7A)	109.5	C(10)-C(11)-C(14)	122.0(3)
C(1)-C(7)-H(7B)	109.5	C(13)-C(12)-C(11)	122.1(3)
H(7A)-C(7)-H(7B)	109.5	C(13)-C(12)-H(12)	118.9
C(1)-C(7)-H(7C)	109.5	C(11)-C(12)-H(12)	118.9
H(7A)-C(7)-H(7C)	109.5	C(12)-C(13)-C(8)	120.0(2)
H(7B)-C(7)-H(7C)	109.5	C(12)-C(13)-H(13)	120.0
C(9)-C(8)-C(13)	119.1(3)	C(8)-C(13)-H(13)	120.0
C(9)-C(8)-N(2)	118.9(2)	C(11)-C(14)-H(14A)	109.5
C(13)-C(8)-N(2)	121.9(2)	C(11)-C(14)-H(14B)	109.5
C(10)-C(9)-C(8)	120.1(3)	H(14A)-C(14)-H(14B)	109.5
C(10)-C(9)-H(9)	120.0	C(11)-C(14)-H(14C)	109.5
C(8)-C(9)-H(9)	120.0	H(14A)-C(14)-H(14C)	109.5
C(9)-C(10)-C(11)	121.5(2)	H(14B)-C(14)-H(14C)	109.5
C(9)-C(10)-H(10)	119.2	C(2)-N(2)-C(8)	126.9(2)
C(11)-C(10)-H(10)	119.2	C(2)-N(2)-H(2)	116.5
C(12)-C(11)-C(10)	117.2(3)	C(8)-N(2)-H(2)	116.5
C(12)-C(11)-C(14)	120.8(3)	C(4)-O(1)-C(1)	109.27(19)

Symmetry transformations used to generate equivalent atoms:

Table 4. Anisotropic displacement parameters ($\text{\AA}^2 \times 10^3$) for **6a**. The anisotropic displacement factor exponent takes the form: $-2p^2[h^2 a^{*2} U^{11} + \dots + 2 h k a^* b^* U^{12}]$

	U^{11}	U^{22}	U^{33}	U^{23}	U^{13}	U^{12}
C(1)	43(1)	14(1)	37(1)	0(1)	12(1)	1(1)
C(2)	43(1)	17(1)	29(1)	-1(1)	14(1)	-1(1)
C(3)	39(1)	20(1)	31(1)	1(1)	12(1)	4(1)
C(4)	44(1)	18(1)	33(1)	2(1)	18(1)	4(1)
C(5)	49(2)	19(1)	37(1)	3(1)	8(1)	-1(1)
C(6)	58(2)	40(2)	41(2)	4(1)	17(1)	-9(1)
C(7)	47(2)	22(1)	53(2)	-4(1)	22(1)	2(1)
C(8)	45(1)	18(1)	30(1)	2(1)	14(1)	-4(1)
C(9)	52(2)	22(1)	36(1)	-2(1)	20(1)	-4(1)
C(10)	58(2)	31(2)	37(1)	-9(1)	20(1)	-17(1)
C(11)	52(2)	36(2)	38(1)	-4(1)	25(1)	-16(1)
C(12)	48(2)	34(2)	46(2)	-6(1)	28(1)	-10(1)
C(13)	51(2)	26(1)	37(1)	-7(1)	21(1)	-8(1)
C(14)	54(2)	61(2)	53(2)	-13(2)	28(2)	-22(2)
N(1)	83(2)	63(2)	56(2)	-6(2)	37(2)	-6(2)
N(2)	46(1)	15(1)	34(1)	-1(1)	12(1)	2(1)
O(1)	42(1)	14(1)	38(1)	-1(1)	12(1)	0(1)
O(2)	52(1)	14(1)	49(1)	0(1)	23(1)	1(1)

Table 5. Hydrogen coordinates ($\times 10^4$) and isotropic displacement parameters ($\text{\AA}^2 \times 10^3$) for **6a**.

	x	y	z	U(eq)
H(3)	3160	4238	10338	36
H(5A)	84	7406	7605	45
H(5B)	1063	8786	8100	45
H(7A)	-352	7430	9122	60
H(7B)	566	8892	9712	60
H(7C)	479	6878	10234	60
H(9)	3554	10608	11547	43
H(10)	5294	11227	12424	49
H(12)	5982	7032	10805	48
H(13)	4251	6453	9893	44
H(14A)	7261	8506	12774	81
H(14B)	7055	10787	12652	81
H(14C)	7295	9613	11790	81
H(2)	2283	9262	9899	39